



Title	Numerical integration approach to the problem of simulating damage in an asphalt pavement
Authors(s)	O'Brien, Eugene J., Taheri, A.
Publication date	2011-06-13
Publication information	O'Brien, Eugene J., and A. Taheri. "Numerical Integration Approach to the Problem of Simulating Damage in an Asphalt Pavement" 13, no. 4 (June 13, 2011).
Publisher	Taylor and Francis
Item record/more information	http://hdl.handle.net/10197/4075
Publisher's statement	This is an electronic version of an article published in International Journal of Pavement Engineering, Volume 13, Issue 4, 2012 . International Journal of Pavement Engineering available online at: http://www.tandfonline.com/doi/full/10.1080/10298436.2011.575135
Publisher's version (DOI)	10.1080/10298436.2011.575135

Downloaded 2023-10-05T14:16:07Z

The UCD community has made this article openly available. Please share how this access benefits you. Your story matters! (@ucd_oa)



© Some rights reserved. For more information

Numerical Integration Approach to the Problem of Simulating Damage in an Asphalt Pavement

E.J. OBrien & A. Taheri

School of Civil, Structural & Environmental Engineering, University College Dublin

Abstract

A road develops permanent deformation or fatigue damage because of the stress and strain induced in its structure by surface loading and environmental change. Dynamic tyre forces generated by the vibration of moving heavy vehicles excited by the road surface profile are strongly influenced by vehicle speed and dynamic properties. A mechanistic-empirical approach is implemented here to simulate the deterioration of a pavement, taking account of dynamic excitation of the axles. This paper highlights the importance of statistical spatial repeatability in damage evolution during the pavement life. Numerical integration of the distribution of forces at each point is shown to be sufficient to predict the changing road surface and elastic modulus. This results in an approximate 100-fold increase in computational efficiency. Finally, the pattern of the forces generated by axles of a half car, are found to be a little less damaging than those of independent quarter cars. In the examples considered, the quarter car reduces calculated pavement life by an average of 6%.

Keywords: Pavement, statistical spatial repeatability, dynamic, truck fleet, mechanistic-empirical, numerical integration.

1. Introduction

Pavements deteriorate in response to forces applied by passing vehicles and as a result of environmental effects [1, 2]. The traditional approach to pavement life assessment considers all axle weights that are anticipated and calculates the number of equivalent axles of standard weight. It does not explicitly calculate the effect of dynamic oscillation of axle forces about the static weight. More significantly, the traditional approach to pavement assessment does not account for 'spatial repeatability', the fact that the mean pattern of dynamic forces applied by a truck to a pavement is repeatable. Many researchers [3-6] have presented evidence showing that for a given speed, the dynamic wheel force time histories generated by a particular heavy vehicle are concentrated and repeated at specific locations along the road for repeated test runs. DePont and Pidwerbesky [7] use dynamic vehicle models in an attempt to generate the mean patterns of dynamic forces. However, they used a stochastic road profile so it is not surprising that they did not get a good match to the measured mean patterns. Cole and Cebon [3] also tried to reproduce patterns of spatial repeatability but did not allow for the variability in the vehicle dynamic properties. This paper uses a computer model which predicts the dynamic behaviour of a truck fleet.

The mechanistic-empirical approach [2, 3, 5, 8-11] is used for assessing the remaining service life of a pavement. The procedure, illustrated in Fig. 1, can be divided into four main areas: dynamic vehicle simulation; pavement primary response calculation; pavement damage calculation and damage feedback mechanism. The inputs to the model are:

- (i) the details of the pavement being simulated (layer thicknesses, mix specifications etc);
- (ii) the initial conditions (road surface profile and material stiffnesses);
- (iii) the traffic loading and
- (iv) the climatic conditions.

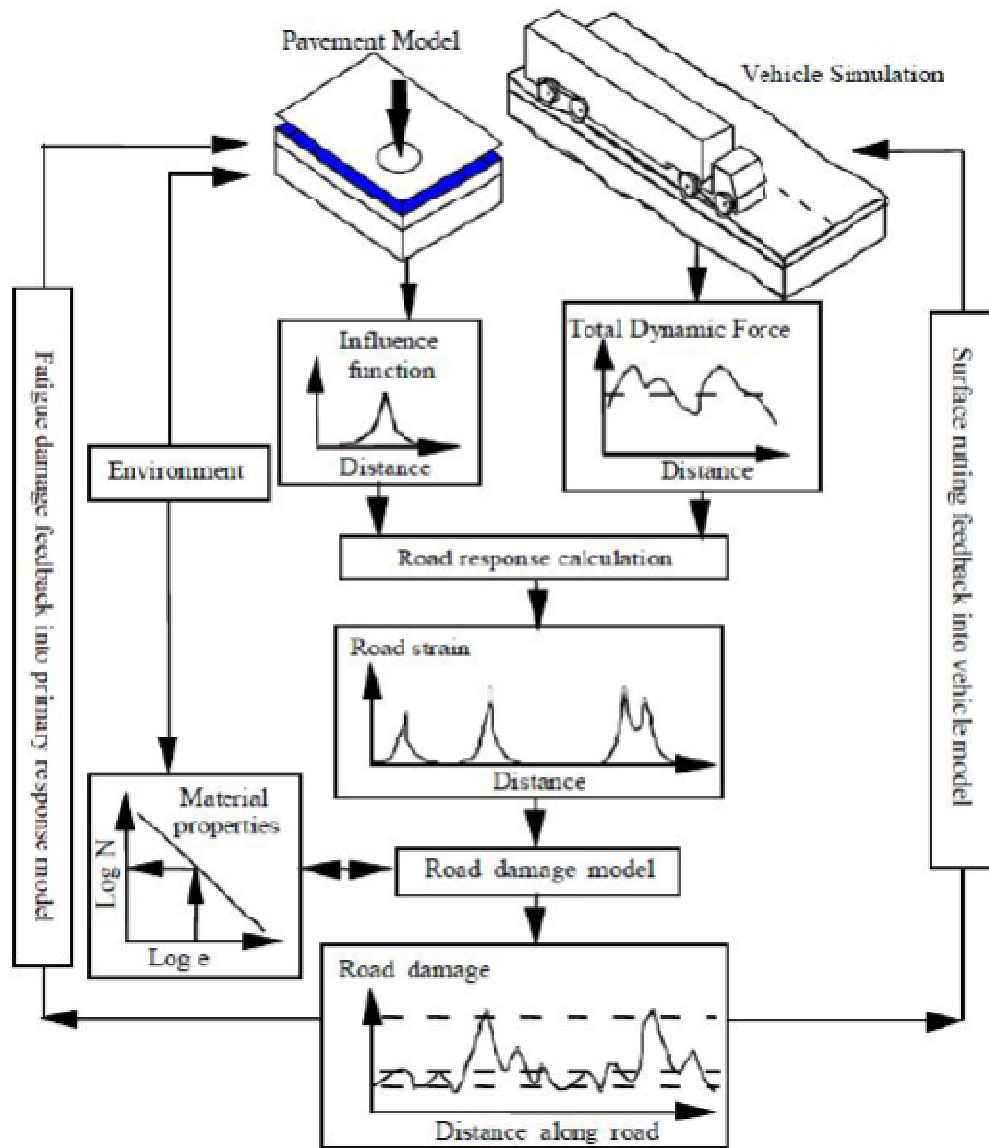


Figure 1 Mechanistic-empirical pavement performance framework [5]

A section of pavement is divided along its length into many equally spaced sub-sections. A time domain vehicle simulation is used to generate dynamic tyre forces for vehicles as a function of distance. Primary response “influence functions” for each pavement sub-section and each mode of damage are used to calculate peak strains as each axle passes. In this implementation of the mechanistic-empirical approach, the simplified Method of Equivalent Thickness [12] is used. For each passing axle, the primary response is combined with the appropriate pavement damage models to predict damage as a function of distance along the pavement. Damage manifests itself in the model in two ways:

1. Rutting has the effect of changing the surface profile (permanent deformation).
2. Fatigue damage reduces the modulus of elasticity. This has the effect of reducing the ability of the pavement to disperse the wheel load, resulting in greater strains for a given load.

An updated surface profile is generated by subtracting the calculated permanent deformation in the wheel path from the profile that existed before the axle passed. This mechanism accounts for the effects of changing surface profile on the excitation of the axle and hence the change in the spatial repeatability pattern of dynamic tyre forces. The process is repeated for millions of axle passes until the pavement has reached the end of its serviceable life. The process of calculating many millions of dynamic responses is computationally very demanding. This paper presents an integration approach which allows for the changing spatial repeatability pattern with orders of magnitude improvement in computational efficiency.

1.1 Failure Model

Fatigue damage is represented in this model through a reduction in the elastic modulus with increasing damage:

$$E = E_0 \exp^{-C_3 D} \quad (1)$$

where E_0 is the initial elastic modulus, C_3 is a constant and D is a damage term given by:

$$D = \sum_{i=1}^j \frac{N^{(i)}}{N_f^{(i)}} \quad (2)$$

The term $N^{(i)}$ is the number of cycles at a given level of tensile strain, ε_i , at the bottom of the asphalt layer and $N_f^{(i)}$ is the number of cycles to failure at that strain level. Fatigue is assumed to do no further damage when the elastic modulus reaches a minimum limiting value of $0.2E_0$.

The permanent deformation due to rutting in the transformed equivalent thickness is calculated from Eq. (3). The incremental rut depth due to a single axle load may be expressed as:

$$\delta = L_1 \varepsilon_c^{L_2} \quad (3)$$

where ε_c is the vertical subgrade compressive strain and L_1 and L_2 are material constants.

Throughout this study, the asphalt thickness, initial elastic modulus, etc. are considered constant along the length of the road profile. However, as the damage is calculated point by point, the Numerical Integration approach is equally applicable to examples where such parameters are

variable. It is anticipated that such variability would affect the damage process in a similar way to the variations in the initial profile.

2. Statistical Spatial Repeatability

The dynamic wheel forces applied by an axle to a pavement depend on road roughness, suspension type and vehicle speed. The concept of spatial repeatability is well established, i.e., as the same truck travels repeatedly over a given stretch of road at approximately the same speed, the pattern of dynamic forces is approximately the same for each run. “Statistical spatial repeatability” (SSR) [13] is the phenomenon that the *mean* pattern of dynamic force applied by a large group of axles to a given stretch of road is also repeatable, i.e., the same approximate *mean* pattern will apply for each group of axles. The phenomenon is illustrated in Fig. 2 which shows mean patterns of measured dynamic wheel forces on a section of road near Arnheim in the Netherlands. Three patterns are illustrated, each representing the mean force applied by the third axle of one thousand 5-axle trucks. SSR has significant implications for pavement damage as some points (e.g., $x = 0$ in Fig. 2) are subject to higher mean forces than others (e.g., $x = 19.5$). It can be inferred that the former point will be more damaged than the latter, unless/until the SSR pattern changes.

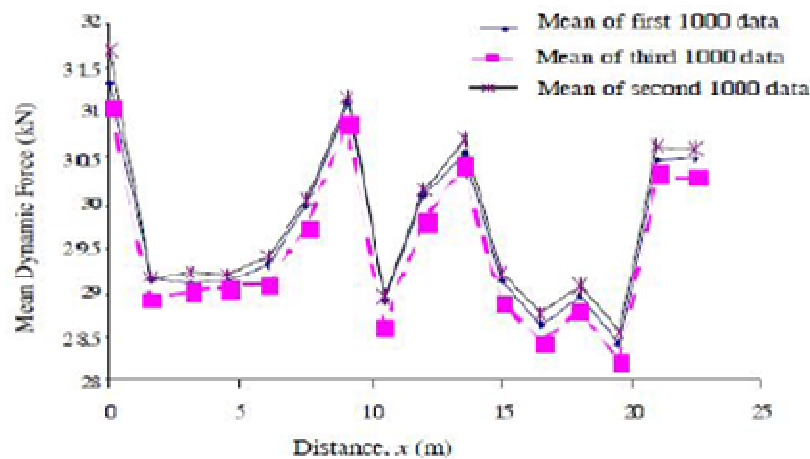


Figure 2 Measured patterns of statistical spatial repeatability

3. Distribution of Forces at Various Points

A truck fleet model differs from a conventional truck dynamic model in that a force pattern is calculated for each of many passing axles. Different combinations of vehicle properties are used in each run, reflecting variations between individual axles on the road. Such a model allows for

statistical variation in the axle properties such as stiffness and mass. The outputs of repeated dynamic calculations are statistical distributions of dynamic force at each point along the road. Wilson et al. [14] use Bayesian updating to find the statistical distributions for a truck fleet model when applied dynamic forces are known, as would be the case with a dynamically calibrated multiple-sensor weigh-in-motion system. They then use the truck fleet model to predict patterns of statistical spatial repeatability.

For the truck fleet models described here, all the vehicle parameter properties are assumed to be Normally distributed. Hence, the distribution of each property can be represented by its mean and standard deviation. A quarter car model is used here with the distribution properties given in Table 1 [2, 10, 15, 16].

Table 1 Parameters of quarter car fleet model

Vehicle parameter	Mean	Standard Deviation
Unsprung mass, m_u (kg)	420	40
Sprung mass, m_s (kg)	4535	500
Suspension stiffness, K_s (N/m)	1 000 000	100 000
Suspension damping, C_s (Ns/m)	20 000	2,000
Tyre stiffness, K_t (N/m)	1 950 000	200 000
Velocity, v (m/s)	22.43	2.40

Monte Carlo simulation is used to calculate the force patterns due to 5000 quarter cars from this fleet on an initially random road surface profile (Fig. 3). The resulting distributions of applied force are illustrated in Figs. 4 and 5. For this example, the most frequent force varies from as low as 48 kN (at $x = 30$ m) to as high as 52 kN (at $x = 10$). The standard deviations also vary with location though not to a great extent.

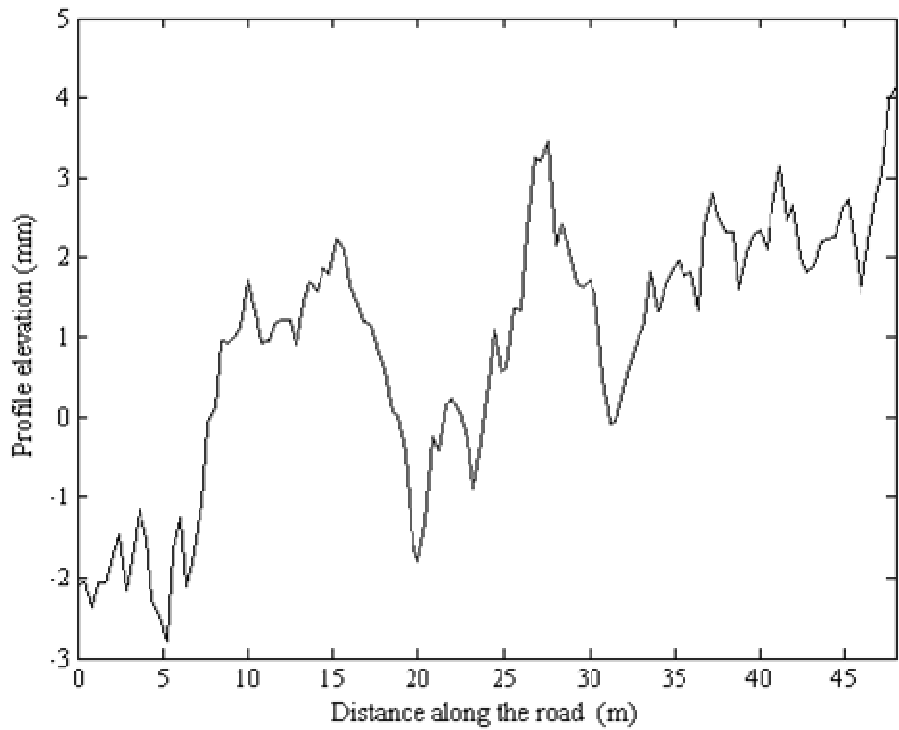
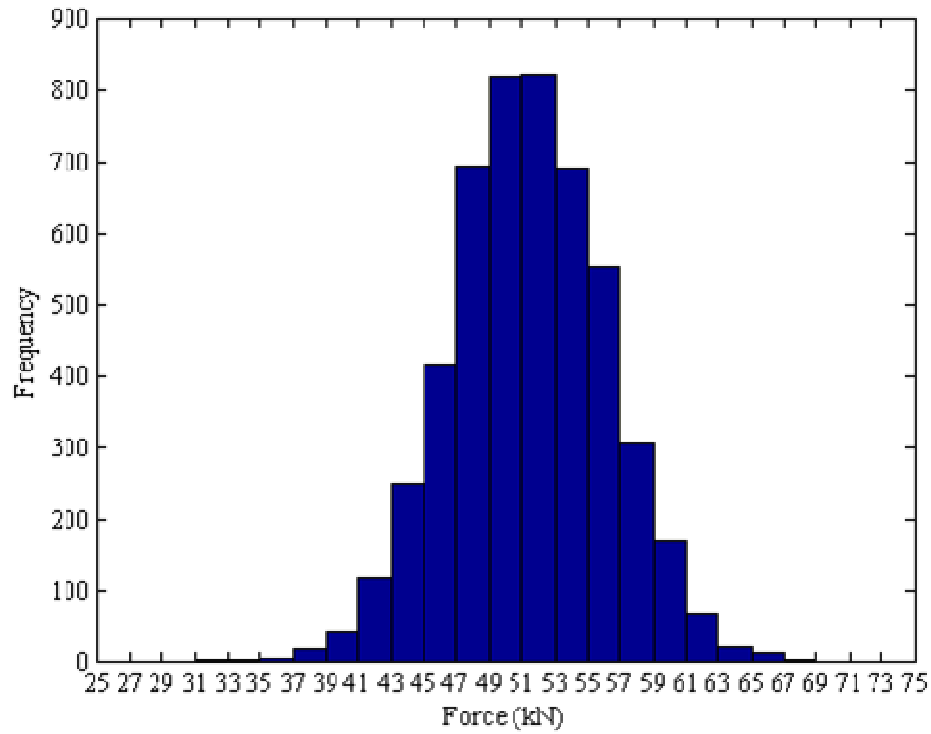
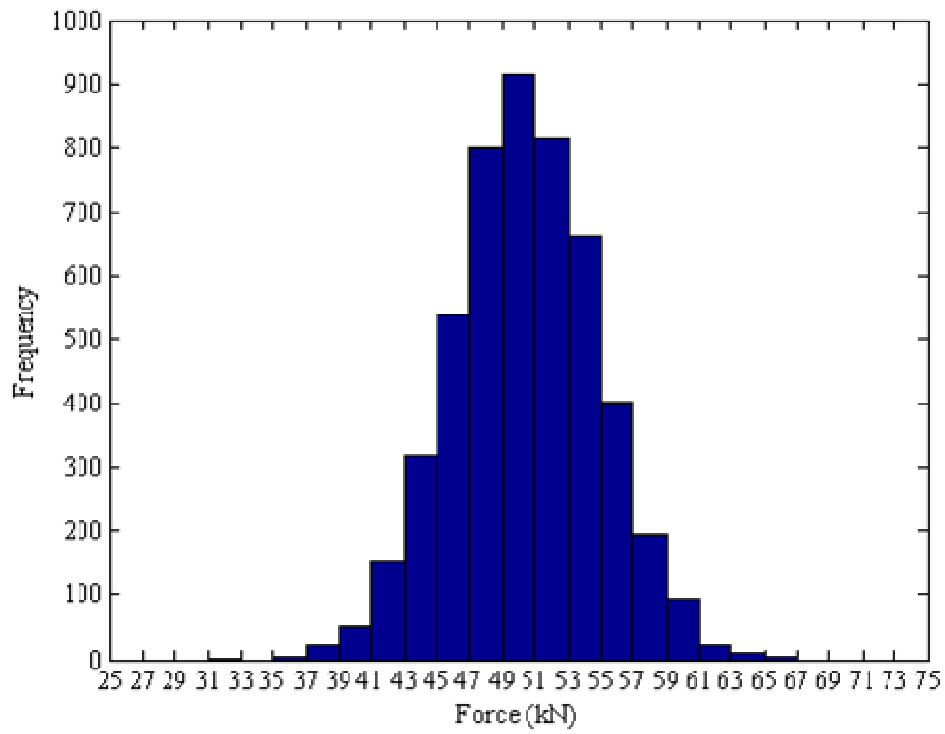


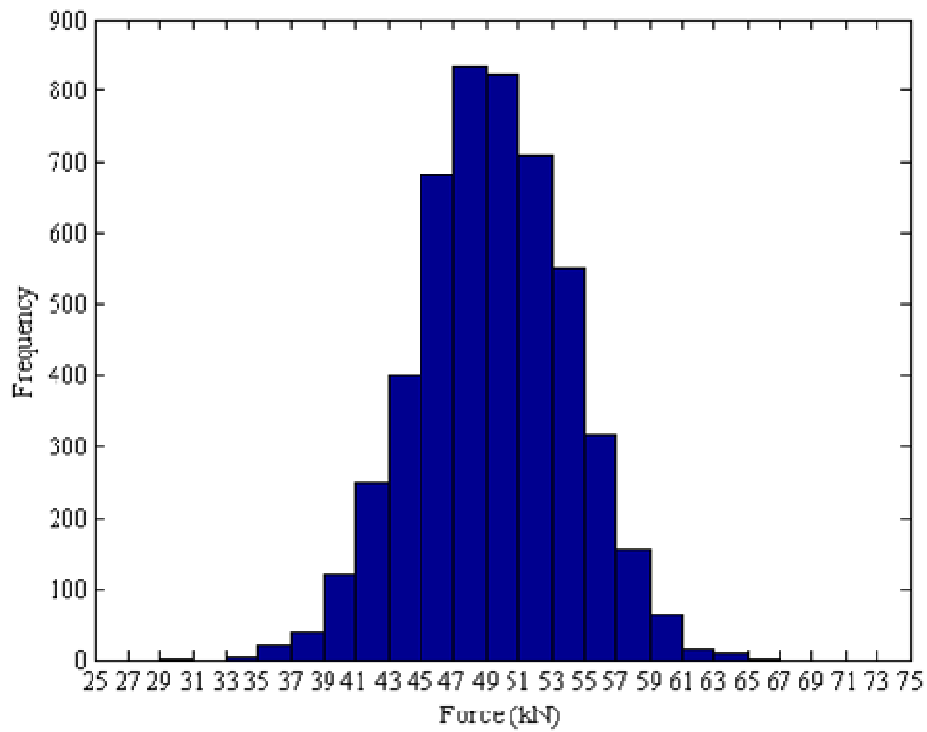
Figure 3 Initial Road Profile



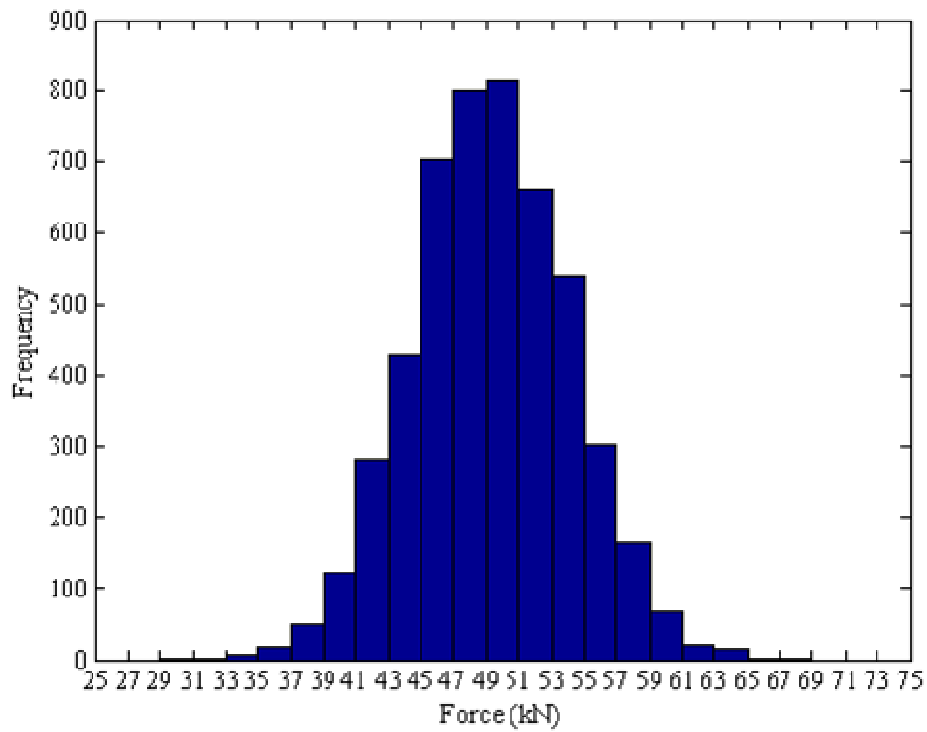
(a) Histogram of force at $x = 10$ m



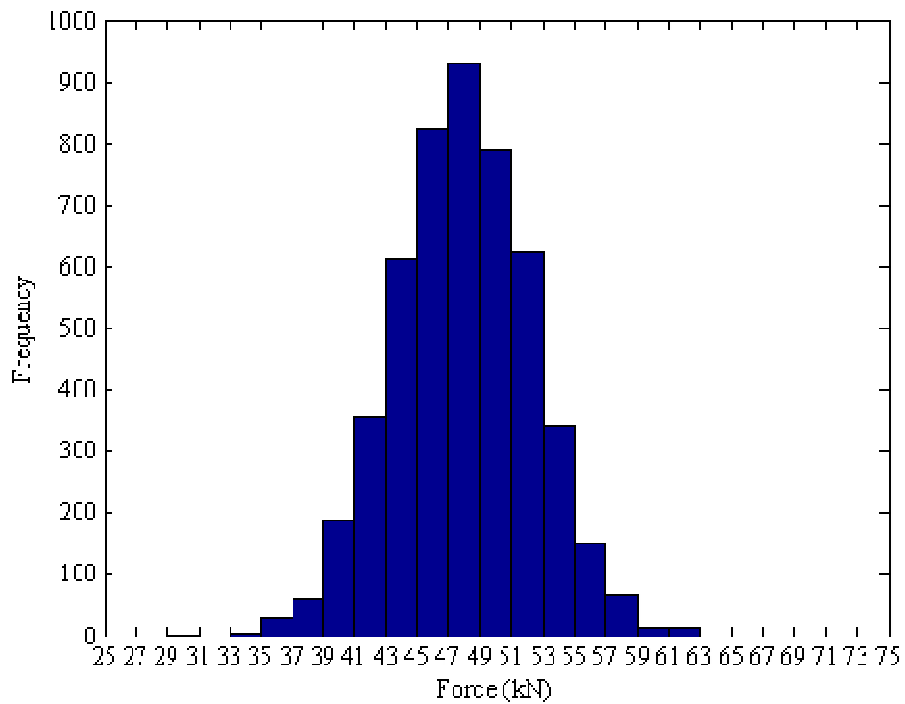
(b) Histogram of force at $x = 15$ m



(c) Histogram of force at $x = 20$ m



(d) Histogram of force at $x = 25$ m



(e) Histogram of force at $x = 30$ m

Figure 4 Histogram of applied dynamic forces at $x = 10, 15, 20, 25$ and 30 m.

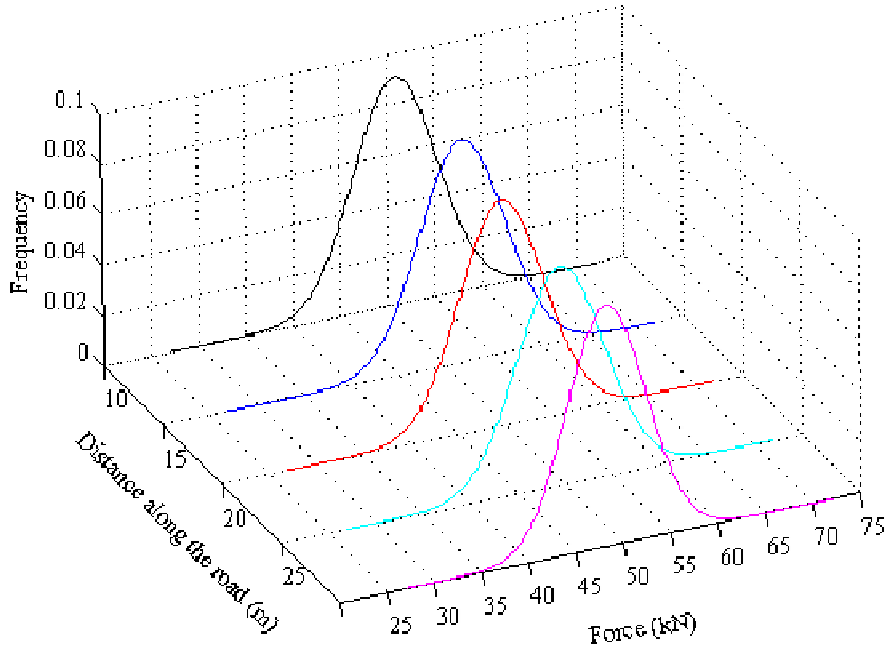


Figure 5 Distributions of force at various points along the road

The differential equations describing the motion of a vehicle are linear and the results can therefore be superposed [17]. A road profile can be discretized and described by a series of n steps of magnitude, s_i , $i = 1, n$ (Fig. 6). Hence, for a fixed (deterministic) quarter car, the force at any point, j , due to excitation of the profile, is the sum of the forces at that point due to each step:

$$F_j = \sum_{i=1}^n f_{ji} s_i \quad (4)$$

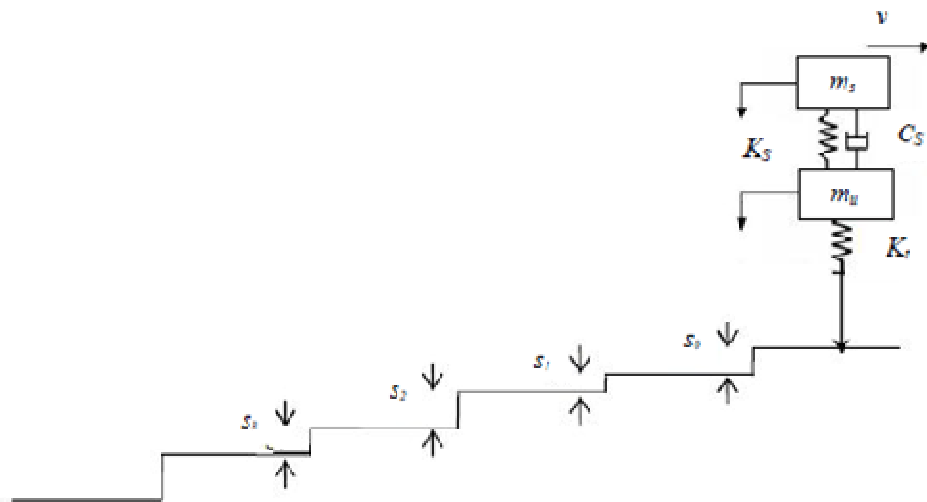


Figure 6 Discretized road profile with quarter car model

where f_{ji} is the force at j due to a unit step at i . For a truck fleet model, the force at j due to a unit step at i is a random variable and the mean force (i.e., mean of the SSR pattern) is given by:

$$\bar{F}_j = \sum_{i=1}^n \bar{f}_{ji} s_i \quad (5)$$

where \bar{f}_{ji} is the mean of the forces at j due to a fleet of quarter cars passing over a unit step at i .

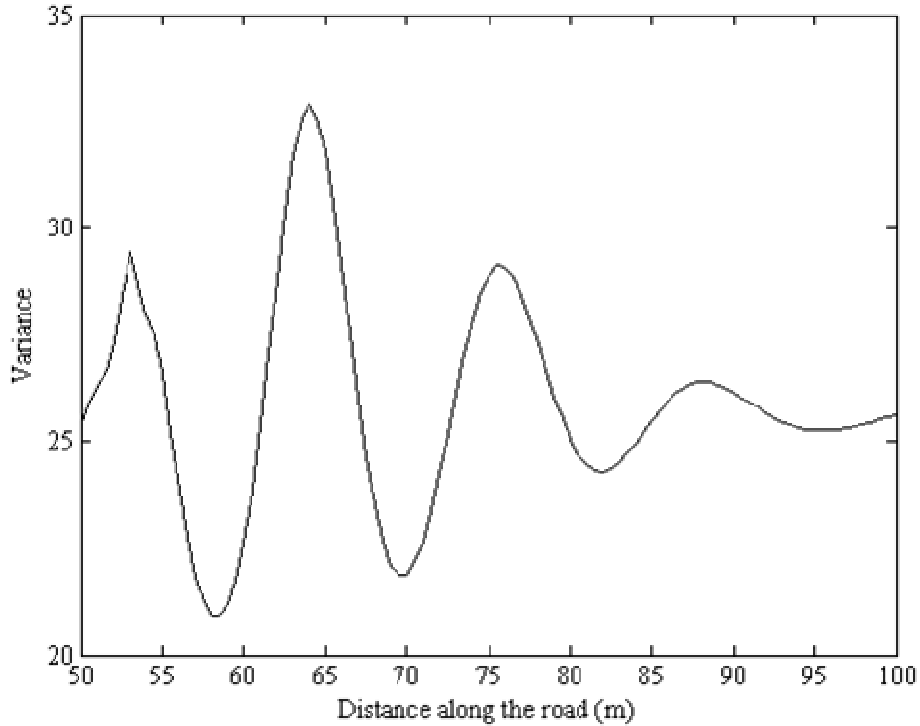
The variance of the applied force is given by:

$$\text{Var}(F_j) = \underline{s}^T [C_j] \underline{s} \quad (6)$$

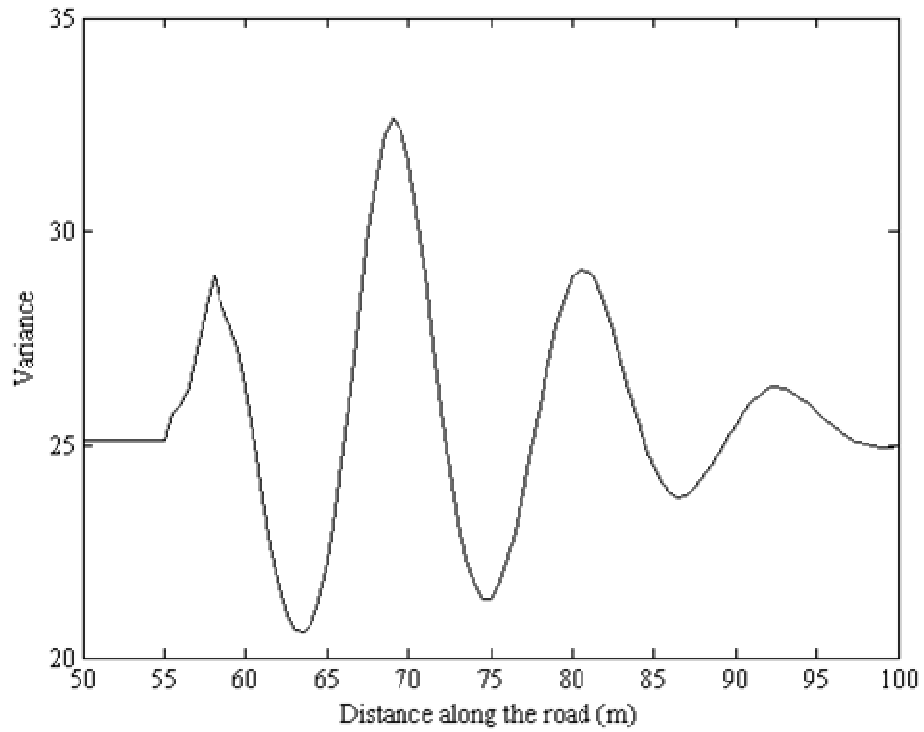
where \underline{s} is the vector of profile steps and $[C_j]$ is a matrix of variances and covariances:

$$[C_j] = \begin{bmatrix} \text{var}(f_{j1}) & \text{cov}(f_{j1}, f_{j2}) & \cdots & \cdots & \text{cov}(f_{j1}, f_{jn}) \\ \text{cov}(f_{j1}, f_{j2}) & \text{var}(f_{j2}) & & & \cdot \\ \cdot & & \cdot & & \\ \cdot & & & \cdot & \text{cov}(f_{j,n-1}, f_{jn}) \\ \text{cov}(f_{j1}, f_{jn}) & \cdots & \text{cov}(f_{j,n-1}, f_{jn}) & \text{var}(f_{jn}) & \end{bmatrix} \quad (7)$$

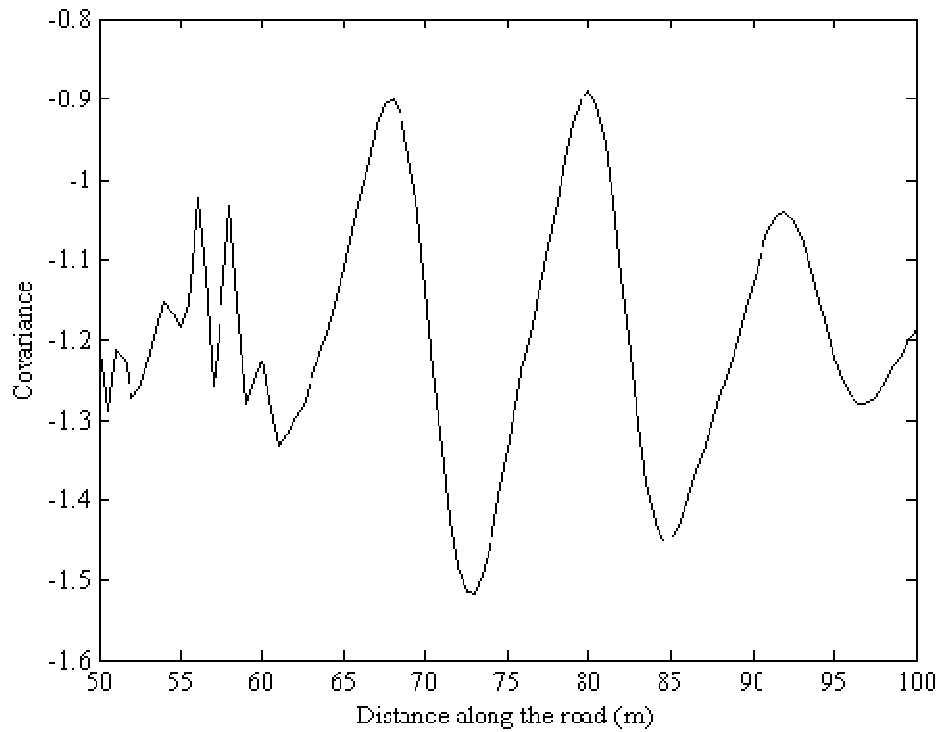
As an example, a profile is considered that is everywhere smooth except for two 5 mm steps, one at $x = 50$ m and one at $x = 55$ m. The variances and covariances for the points, j , right of these steps are illustrated in Fig. 7.



(a) Variances of the dynamic forces due to a unit step at $x = 50$ m



(b) Variances of the dynamic forces due to a unit step at $x = 55$ m



(c) Covariances between the forces generated by the two steps, $\text{cov}(f_{j1}, f_{j2})$

Figure 7 Variances and covariances of forces at various points due to a simple road profile with two step changes

For this example the covariances are negative, with magnitudes that vary with the point j considered. It can be seen that with steps this distance (5 m) apart, the magnitudes of the covariances are generally small. However, for profiles with many steps, there are far more covariance than variance terms in Eq. (6). Furthermore, for steps near each other, the covariance terms will be significantly greater. Hence, their contribution cannot be neglected in a calculation of force variance. In general, a profile might be discretized at, for example, 0.1 m intervals and the $[C_j]$ matrix becomes very large. A numerical approach is therefore adopted to determine the force distributions (as opposed to solving Eqs. (5) and (6)).

4. Road damage calculation by numerical integration

Mechanistic-empirical design is complicated by the feedback loop in the road profile, i.e., the pattern of forces causes rutting which changes the initial profile which in turn changes the pattern of forces. Fortunately these changes are small and it is proposed here to assume that there is no significant change for all axles that pass in one week. This corresponds to about 100 000 axles on a busy highway. The 1 week interval is also suitable for incorporating small increments of seasonal temperature change. The approach is illustrated in Fig. 8. The statistical distributions of force at each point are estimated from a simulation of 1000 axles. The damage, both rutting and fatigue, is then calculated by numerical integration over the full range of recorded forces at each point, using a histogram with bins at 2 kN intervals. The resulting damage is scaled to determine the damage due to all axles that pass in the week. The road profile and elastic moduli and the climatic conditions (temperature) are updated after each week and the process repeated until the pavement fails. The effect of this approach is an approximate 100-fold improvement in computational efficiency with minimal loss of accuracy.

4.1 Step Road Profile with Quarter Car Model

To illustrate the process of pavement damage evolution, a simple initial profile is considered that is perfectly smooth except for a 10 mm step change at $x = 4$ m that is subjected to 15 million passes of the quarter car (Fig. 9 (a)). This is analysed first using the ‘exact’ method, i.e., pavement damage is calculated and the profile updated after the passage of every individual quarter car. It is also analysed using the ‘numerical integration’ approach described above, assuming 100,000 axles per week. The run time for the numerical integration approach was 0.94% of that required for the exact method.

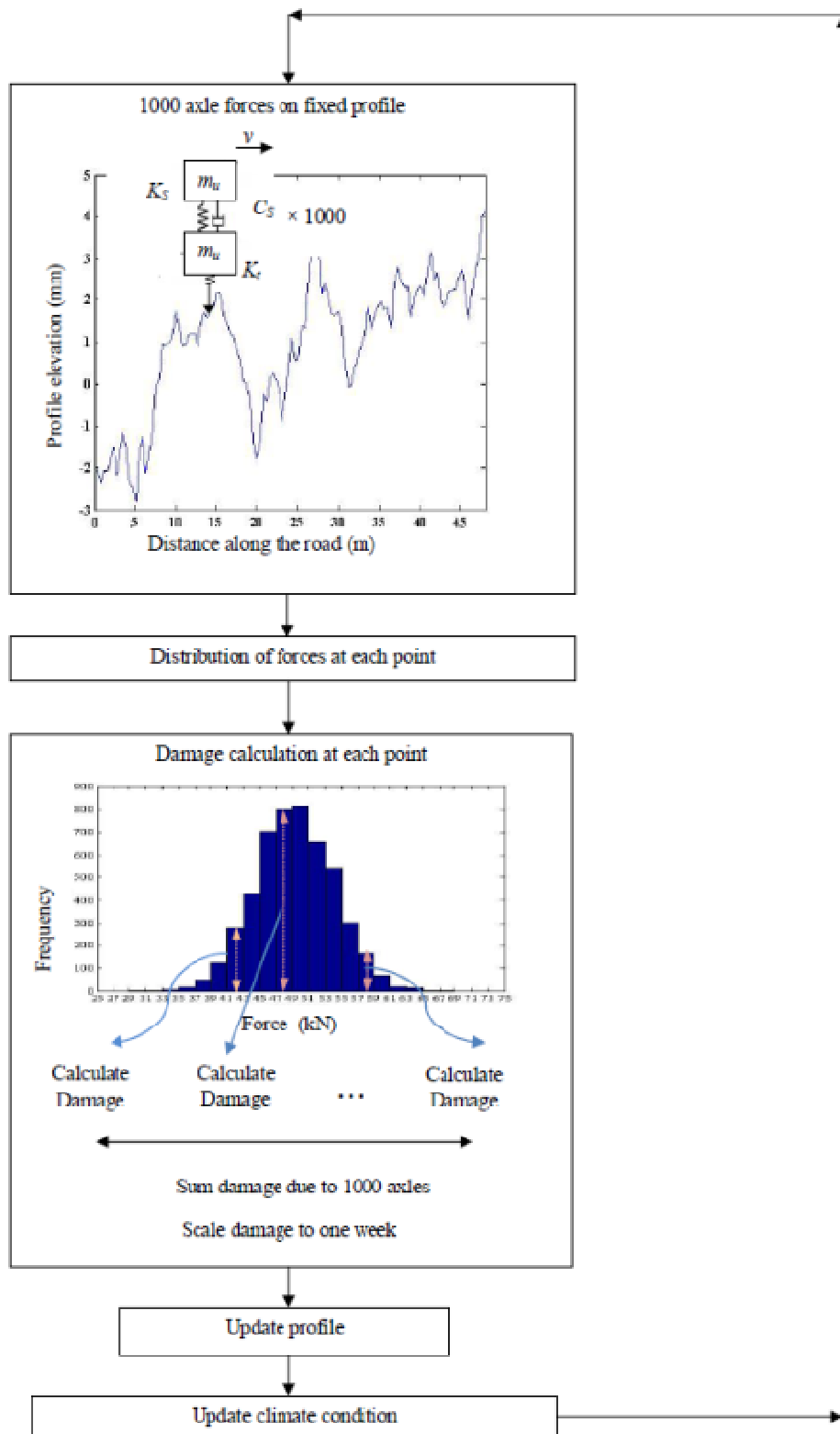
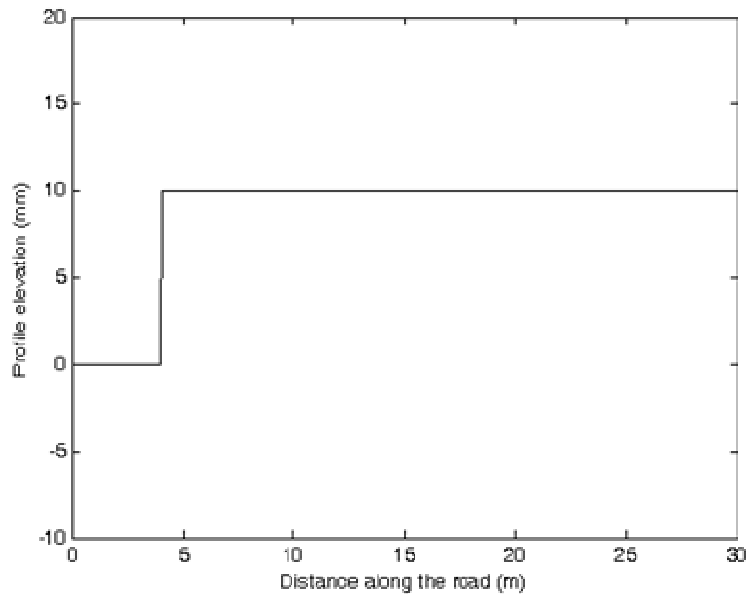


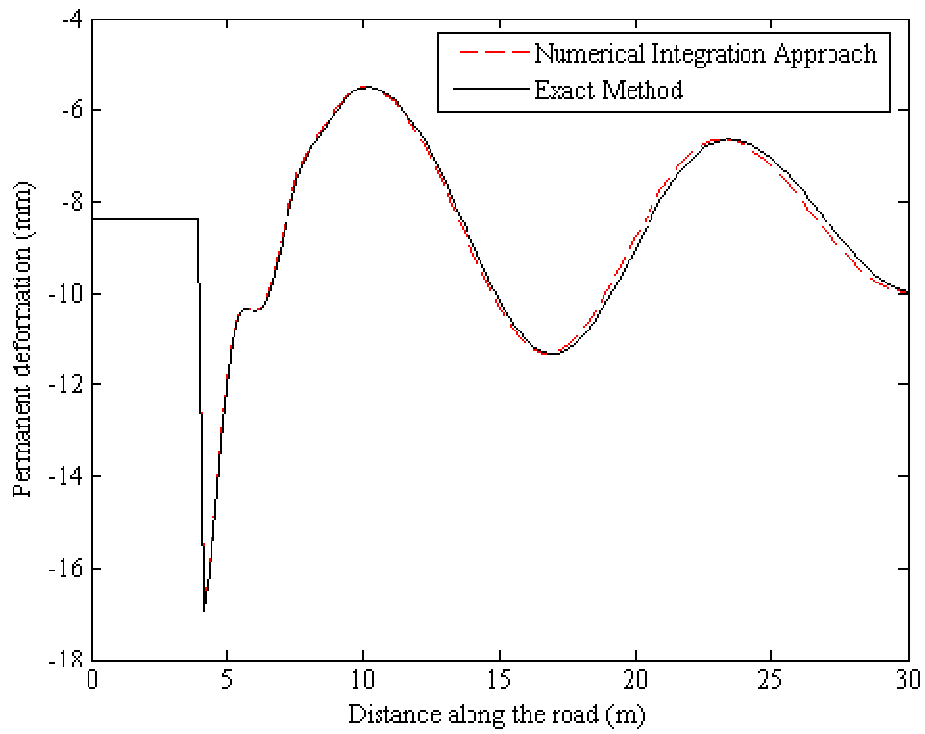
Figure 8 Numerical Integration Approach Framework

The pavement has an asphalt thickness of 0.20 m. The modulus of elasticity of the asphalt layer is calculated assuming typical properties: monthly air temperature range 4°C to 10°C , void content 10%, binder content 3.5%, Specific Gravity of binder 2700 kg/m^3 , Specific Gravity of aggregate 1020 kg/m^3 , proportion of binder 7.9%. The granular layer has a modulus of elasticity of 400 MPa and is 0.2 m thick. The subgrade layer is assumed to be infinitely thick with a modulus of 40 MPa [6]. The Poisson's Ratio is taken to be 0.35 for all three layers (asphalt, granular and subgrade). The permanent deformation of the profile, after 15 million axle passes, is illustrated in Fig. 9(b). It can be seen that there is very little difference in the results, confirming the accuracy of the numerical integration approach. Two frequencies are apparent, corresponding to the two mean frequencies of the fleet of quarter cars. The tyre hop causes greatest damage and has greatest influence immediately adjacent to the step. The lower body frequency corresponds to the suspension. It can be seen to cause damage over a greater extent of road but of lesser magnitude. There are some locations (e.g., $x = 10\text{ m}$) where permanent deformation is less than for static loading alone, i.e., the axle dynamics actually reduces the rutting damage.

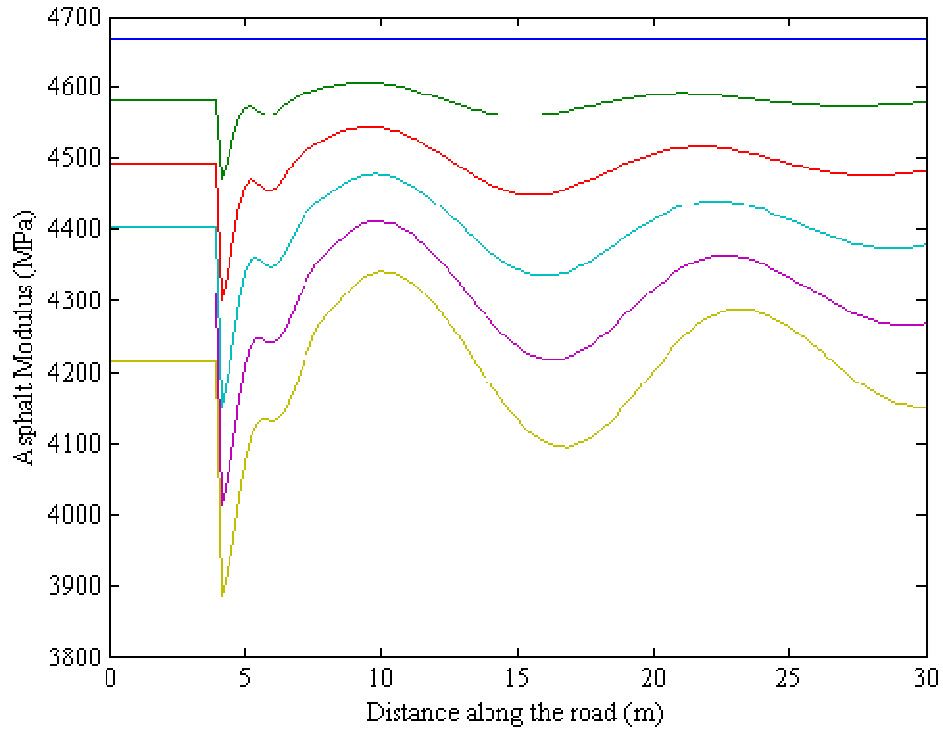
The changing patterns of pavement stiffness are illustrated in Fig. 9 (c). Fatigue damage causes a reduction with increasing number of axle passes. The reduction is most pronounced at $x=4$, where the applied forces, and hence the strains, are greatest.



(a) Initial step profile



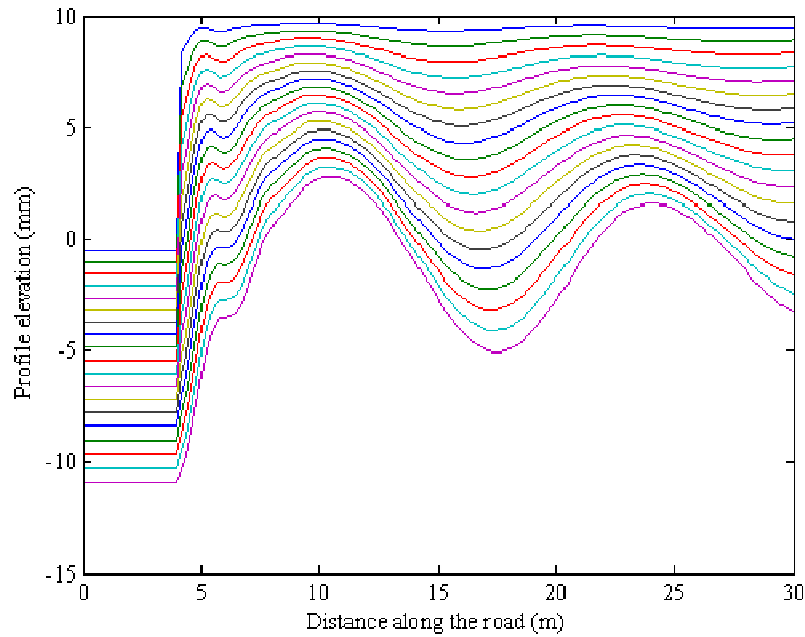
(b) Permanent deformation after 15 million axles



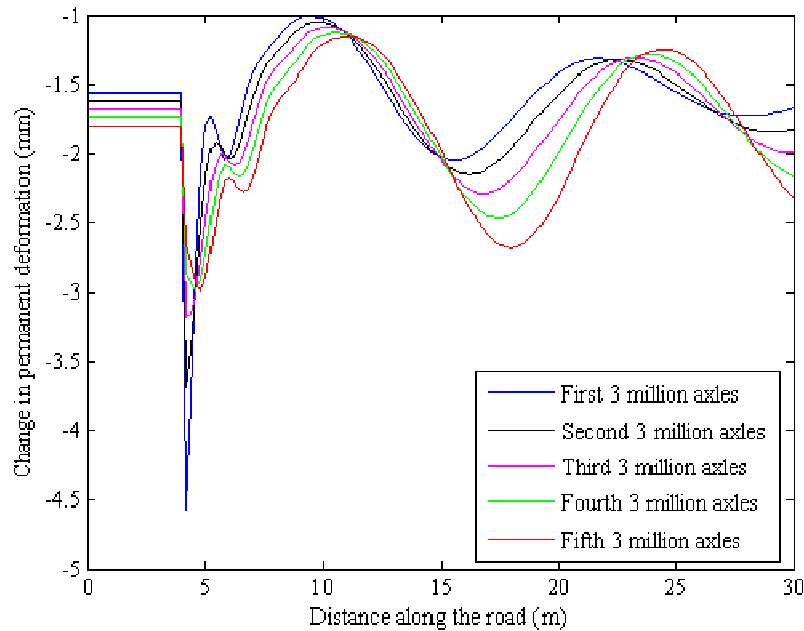
(c) Elastic modulus evolution at intervals of 3 million axles

Figure 9 Progress of road damage over time

The evolution of the pavement profile during its life is illustrated in Fig. 10. The rate of damage increases progressively with time (Fig. 10(b)). This is due to the reduction in the material moduli of elasticity and increasing dynamic forces.



(a) Profile evolution in intervals of 1 million axles



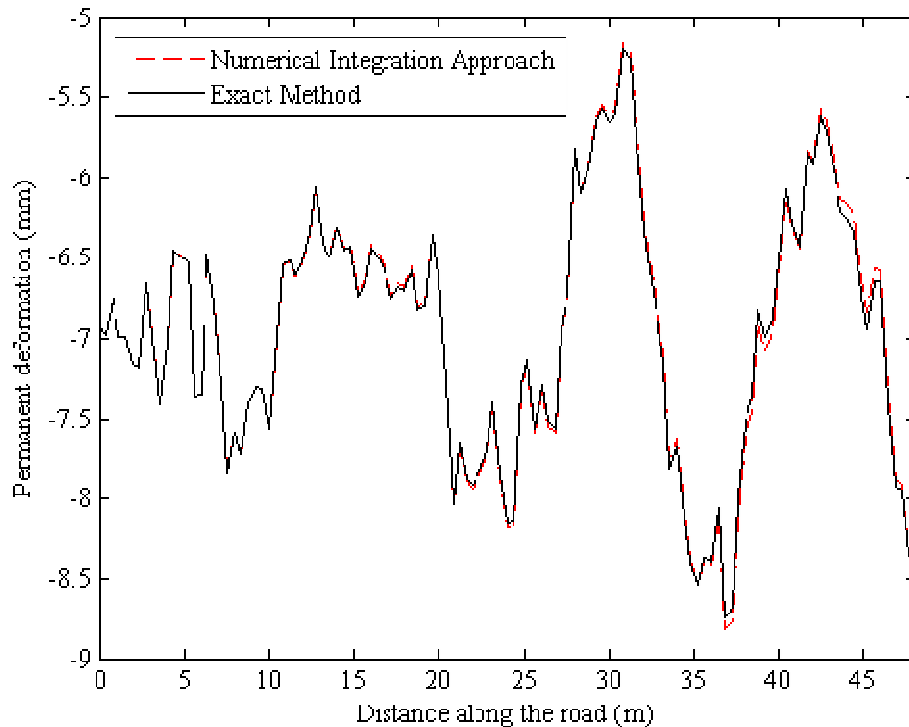
(b) Changes in permanent deformation

Figure 10 Evolution of pavement profile during its life (exact method)

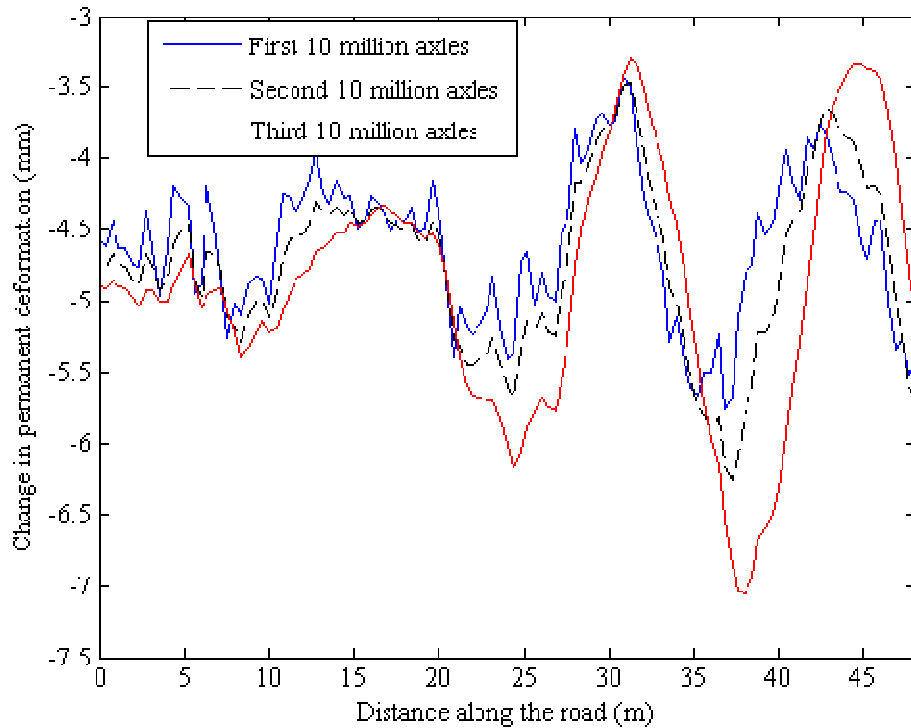
It can also be seen that the locations of the peaks and troughs in the road profile move during its lifetime. For example, a slight trough at about $x = 15$ m in the early stages becomes a significant trough at $x = 17$ m later in the pavement's life.

4.2 Artificially Generated Initial Road Profile with Quarter Car Model

The fleet of quarter cars is also tested on the 50 m length of randomly generated initial road profile illustrated in Fig. 3. The same pavement thickness and material properties are assumed and the same quarter car fleet properties are used as those described above. The numerical integration approach is applied as for the previous example, with updating of the road profile and hence the modulus of elasticity, at weekly (100,000 axle) intervals. It can be seen in Fig. 11(a) that the changes in the profile as calculated using the numerical integration approach, compare very well to the exact method. Fig. 11(b) shows the change in profile due to the 1st, 2nd and 3rd group of 10 million axles. In general, the increment of damage increases for each 10 million group, as the elastic moduli are reducing and the profile is getting rougher. For example, at $x = 35$ to 40 m, the increment of permanent deformation can be seen to be increasing. There are other points where this is not the case. For example, at $x = 45$ m, the increments of permanent deformation are getting smaller. This is because the pattern of statistical spatial repeatability is changing and the peak in the mean force is progressively moving away from this point.



(a) Comparison of permanent deformation



(b) Changes in permanent deformation (exact method)

Figure 11 Permanent deformation for randomly generated Class A initial profile

4.3 Pavement Damage Evolution with Half Car Model

While a quarter car model is commonly used in Mechanistic-empirical analyses of pavement damage, it is clearly preferable to consider more sophisticated vehicle models. There are many types of truck in the fleet at a given site with significantly differing properties. A typical fleet will include mixtures of single, double and supersingle tyres; air and steel suspensions and fixed and articulated suspensions. A change in articulation will influence the pattern of spatial repeatability as it introduces rocking motions between axles.

As an example of a vehicle model, a half car is considered here for the two examples described above. The half car, illustrated in Fig. 12, consists of two quarter cars which are connected through a shared translation and an inter-axle rotation. The properties which define the motion of the axles are all assumed to be Normally distributed with the means and variances given in Table 1. In addition, the vehicle properties of Table 2 are adopted, and a database of gross weights which were measured at a weigh-in-motion site in the Netherlands [16].

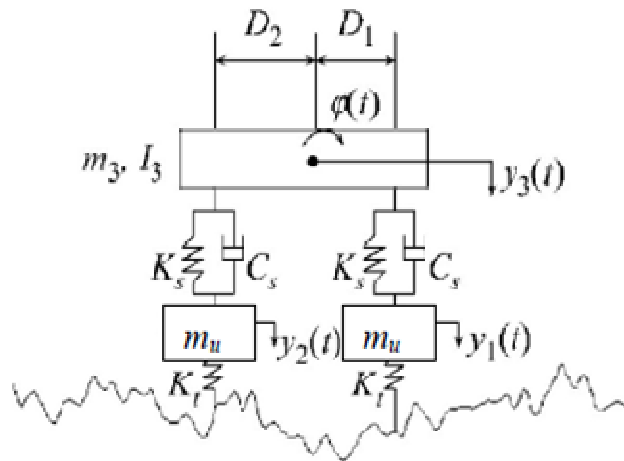


Figure 12 Half Car Model

Table 2 Half Car Fleet Properties

Parameter	Mean Value	Standard Deviation
m_3 (kg)	9065	1875
D_1 (m)	2.675	0.9
D_2 (m)	2.675	0.9
I_3 (kgm ²)	35 300	3 530

As for the quarter car fleet calculations, the half car model is run 1000 times to find the patterns of statistical spatial repeatability, using the initial profile of Fig. 3 and the same pavement properties as before. In this case, histograms at all points are found for each axle separately. As before, numerical integration is used to find the damage due to 1000 vehicles, this time combining the contributions from each axle. The results are then scaled to the total damage in 1 week, assuming 50,000 vehicles (100,000 axles) per week. The profile and the elastic moduli are updated each week and the process repeated until failure of the pavement. As for the previous examples, good agreement is achieved with the exact approach. Fig. 13 shows that the pattern of mean forces for the rear axle is different but similar to the corresponding pattern for the front axle. This difference comes from the pitch of the vehicle which transfers load between axles. More importantly, the mean force pattern for half axles is significantly different from that of the quarter car - see for example, $x = 35$ m. The pitching motion introduces a new frequency which appears to interfere with, and generally reduces the amplitude of, the mean quarter car force pattern. This has significant implications for pavement damage - quarter car models would appear to overestimate the SSR effect.

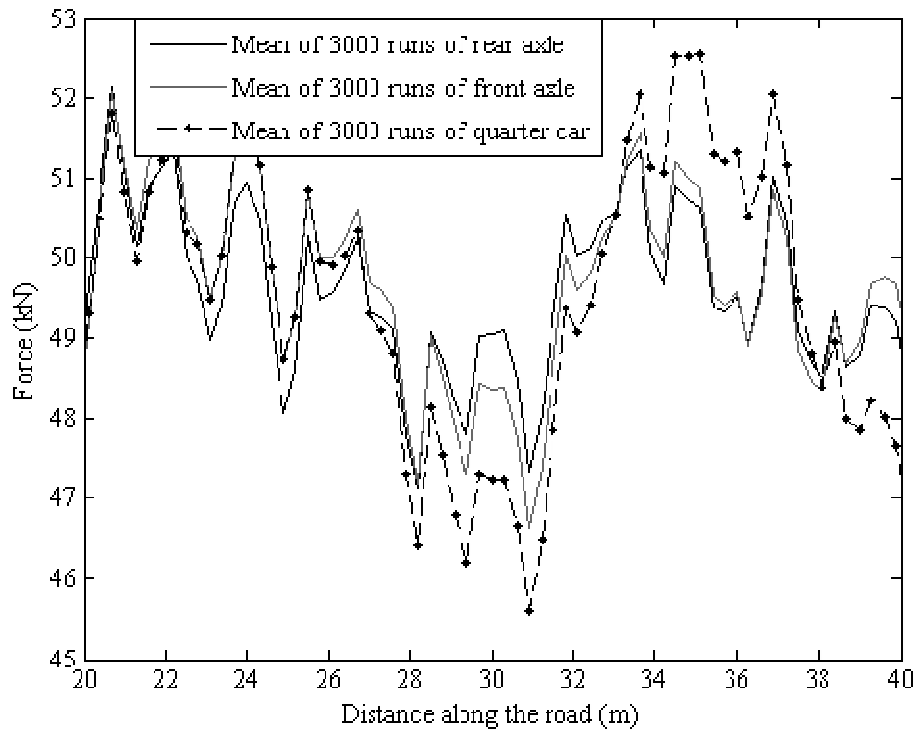


Figure 13 Comparison of mean statistical spatial repeatability pattern for half car and quarter car models after 3000 runs

Fig. 14 compares the damage in the step road profile of Fig. 9(a) between the quarter car and half car models. The body unsprung mass frequency is clear in the road subject to the quarter car fleet, but has been interfered with, in the road subject to the half car fleet. The implications for pavement deformation are illustrated in Fig. 15, which shows significantly less damage due to the half car fleet model.

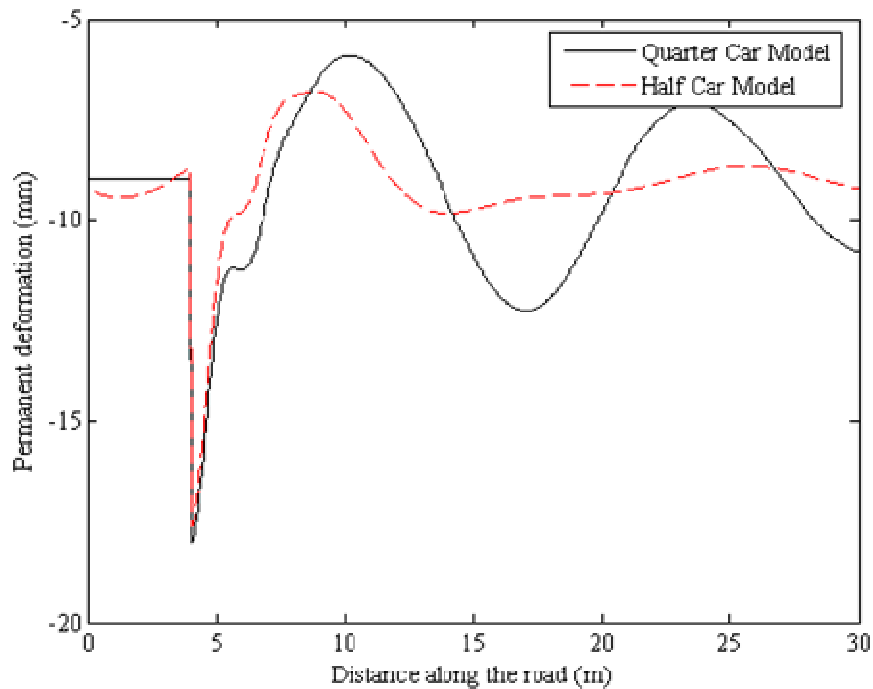


Figure 14 Comparison of permanent deformation between half and quarter car models after 15 million axles

To quantify the influence of the vehicle / axle model on pavement life, eight different initial road profiles of class A, were randomly generated and the Numerical Integration Method applied for both the quarter car and half car models. Table 3 gives the number of axles required to cause failure of the pavement. For this exercise, failure is defined as when the permanent deformation reaches 20 mm or the reduction in stiffness reaches 20 %, whichever happens first. For all eight examples, the half car model requires more axles to cause failure, with an average difference of 6 %.

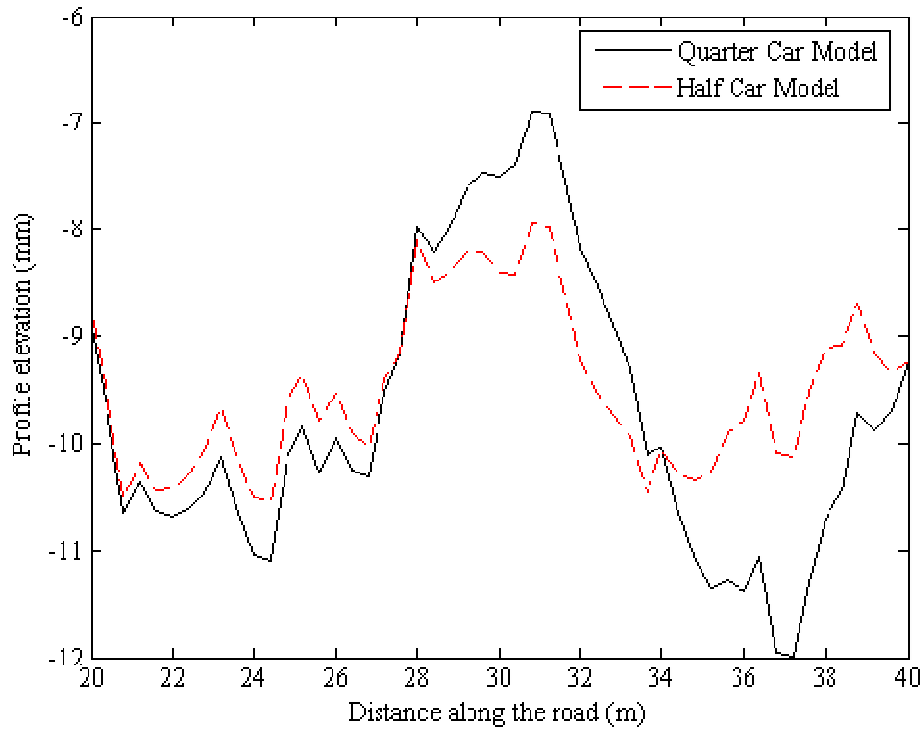


Figure 15 Comparison of permanent deformation between quarter and half car models after 10 million vehicles (20 million axles)

Table 3 Comparison of the number of axles to failure for half and quarter car model

Profiles	Axles to failure (million)		Difference (%)
	Half car	Quarter car	
1	24.2	22.3	7.9
2	24.6	23.6	4.1
3	25.8	24.6	4.7
4	24.7	23.8	3.6
5	25.0	23.2	7.2
6	24.4	22.6	7.4
7	23.5	21.6	8.1
8	25.1	24.1	4.0

5. Conclusions

The statistical distribution of the pattern of dynamic force along a flexible pavement is a key factor in its design or assessment. The Mechanistic-Empirical method requires predictions of the

distribution of dynamic load caused by the fleet of trucks that travels on that section of road. The predicted mean pattern of dynamic force needs to be recalculated periodically as pavement damage causes the road profile to change. The process of calculating many millions of dynamic responses is computationally demanding. This paper presents a method of predicting the statistical distribution of forces, and hence the changing road profile numerically. For a number of examples, 1000 runs of axles or vehicles are found to be sufficient to accurately determine the changing distributions of force at each point. The improvement in computational efficiency is of two orders of magnitude (about 100 fold). Dynamic interference between axles is shown to reduce the mean dynamic force applied by a quarter car model. For eight randomly generated profiles, the quarter car (single axle) model is shown to underestimate the number of axles to cause failure, by an average of 6 % relative to a half car model.

Acknowledgements

The authors wish to acknowledge the support received from the European Framework Project ASSET (Advanced Safety and Driver Support in Efficient Road Transport) and Rijkswaterstaat is thanked for the use of weigh in motion data.

References

- [1] H.F. Southgate, R.C. Deen, *Effects of load distributions and axle and tyre configurations on pavement fatigue*, University of Kentucky, Research Report UKTRP-85-13, 1985.
- [2] D. Cebon, *Handbook of vehicle-road interaction*, Swets and Zeitlinger Publishers, 1999.
- [3] D.J. Cole and D. Cebon, Spatial repeatability of dynamic tyre forces generated by heavy vehicles, *J. Automobile Engineering*, I. Mech. E, Part D, 206, 17-27, 1992.
- [4] T.D. Gillespie, Effects of heavy vehicle characteristics on pavement response and Performance, *Transport Research Board*, No. 353, 1993.
- [5] A.C. Collop, D. Cebon, Parametric study of factors affecting flexible pavement performance, *Journal of Transportation Engineering*, vol. 121, pp. 485-494, 1995.
- [6] M.S.A. Hardy, D. Cebon, The importance of speed and frequency in flexible pavement design, *Journal of Engineering Mechanics*, vol. 120, pp. 463-482, 1994.
- [7] J. DePont, B.D. Pidwerbesky, The impact of vehicle dynamics on pavement performance, *4th International Symposium on Heavy Vehicles Weights and Dimensions*, Ann Arbor, Michigan, Ed. C.B. Winkler, University of Michigan Transportation Research Institute, 1995.
- [8] K. Yi, J.K. Hedrick, Active and semi-active heavy truck suspensions to reduce pavement damage, *SAE Technical paper series*, Technical Report 892486, 1989.
- [9] E. ElBeheiry, D.C. Karnopp, Optimal control of vehicle random vibration with constrained suspension deflection, *Journal of Sound and Vibration*, vol. 189, pp. 547-564, 1996.
- [10] L. Sun, T.W. Kennedy, Spectral analysis and parametric study of stochastic pavement loads, *Journal of Engineering Mechanics*, vol. 128, pp. 318-327, 2002.
- [11] G. Arnold, B. Steven, D. Alabaster, A. Fussell, Effects on pavement wear of increased mass limits for heavy vehicles, stage 3, *Land Transport New Zealand Research*, Report 279, 2005.

- [12] P. Ullidtz, B.K. Larsen, Mathematical model for predicting pavement performance, *Transportation Research Board*, Washington D.C. 949, 1983.
- [13] T. O'Connor, E.J. O'Brien, B. Jacob, An experimental investigation of spatial repeatability, *International Journal of Vehicle Design*, vol. 7, No.1, pp. 64-81, 2000.
- [14] S.P. Wilson, N.K. Harris, E.J. O'Brien, The use of Bayesian statistics to predict patterns of spatial repeatability, *Transport Research C - Emerging Technologies*, vol. 14, pp. 303-315, 2006.
- [15] S. Grave, *Modelling of site-specific traffic loading on short to medium span bridges*, PhD thesis, Trinity College Dublin, 2001.
- [16] E.J. O'Brien, B. Enright, Modeling same-direction two-lane traffic for bridge loading, *Structural Safety*, in press, 2011.
- [17] Y. Li, E.J. O'Brien, A. González, The development of a dynamic amplification estimator for bridges with good road profiles, *Journal of Sound and Vibration*, vol. 293, pp. 125 -127, 2006.